

Received 17 November 2025, accepted 25 December 2025, date of publication 1 January 2026,  
date of current version 6 January 2026.

Digital Object Identifier 10.1109/ACCESS.2025.3650253

## RESEARCH ARTICLE

# Cloud-Based Digital Twins for Vehicle Dynamics Control With Application to Lateral Stability Enhancement

PHILIPP MANDL<sup>1</sup>, JOHANNES EDELMANN<sup>1</sup>, MANFRED PLÖCHL, AND FLORIAN KLINGER

Institute of Mechanics and Mechatronics, TU Wien, 1060 Vienna, Austria

Corresponding author: Philipp Mandl (philipp.mandl@tuwien.ac.at)

This work was supported in part by the Project “Central System for Supporting Automated Vehicle Testing and Operation” by Austrian Research Promotion Agency (FFG) (projekte.ffg.at/projekt/4105771), and in part by TU Wien Bibliothek for Financial Support Through its Open Access Funding Programme.

**ABSTRACT** Vehicle-to-Everything communication facilitates the creation of real-time, cloud-based traffic Digital Twins (DTs) that integrate diverse data streams to offer immediate and predictive insights into the driving environment. Although the application of traffic DTs for automated driving has been extensively studied, their potential to enhance vehicle dynamics control in manually driven vehicles remains underexplored. This paper addresses this gap by investigating the application of cloud-based traffic DTs for vehicle dynamics control. It presents key DT considerations such as model fidelity, data integration, and validation and verification, while exploring prospective DT services and cloud-based control’s inherent advantages and challenges. To illustrate these concepts, a use case for lateral vehicle stability control is presented and experimentally validated. The demonstration shows that using DT-derived information, Adaptive Cruise Control (ACC) and Torque Vectoring (TV) systems can proactively modify vehicle speed and torque distribution to maintain or improve stability and vehicle handling for human drivers. The paper concludes by evaluating the cloud execution of ACC and TV, highlighting the potential to reduce onboard computational requirements.

**INDEX TERMS** Adaptive cruise control, cloud control, cyber-physical system, digital twin, torque vectoring, vehicle dynamics.

## I. INTRODUCTION

Big data is increasingly omnipresent in the automotive sector through Vehicle-to-Everything communication. This connectivity between vehicles, infrastructure (e.g., cameras, traffic lights), and third-party providers (e.g., weather data services, mapping platforms) creates dense networks that share real-time traffic, environmental, and vehicle data. This wealth of data enables the creation of traffic Digital Twins (DTs) – dynamic, virtual replicas of the physical traffic network [1]. While traffic DTs offer significant potential for simulating, monitoring, and optimising traffic scenarios, particularly for autonomous driving [2], contextual information, especially predictive insights from the driving

environment (e.g., road friction potential, road curvature), can benefit lower-level vehicle functions like chassis control [3]. This latter application, however, remains sparsely researched.

Research on traffic DTs, such as the “Central System” [4] and “MCity” [5], enables the development of cloud-assisted and cloud-controlled advanced driver assistance systems services. To achieve real-time operation and maintain up-to-date data, [4] used the public 5G network for Vehicle-to-Everything communication and integrated pedestrian detection from infrastructure cameras, creating an accurate representation of the driving environment.

Implementing real-time traffic DTs entirely onboard a vehicle is impractical due to the substantial data volume, computational power, and bandwidth demands. Consequently, approaches as presented in [4] favour cloud-based architectures, deployed in distributed edge clouds

The associate editor coordinating the review of this manuscript and approving it for publication was Valentin Ivanov.

to utilise the scalability of cloud infrastructure, forming a cyber-physical system.

Concerning the application of DTs for road vehicle dynamics, a recent review by authors in [1] shows that DT applications primarily focus on predictive maintenance, connected and automated road vehicles, and advanced driver assistance systems. Two approaches are emerging for DT-enhanced vehicle dynamics control.

The first is the cloud-based approach, which enables the vehicle-to-cloud (V2C) system of [6] used for cooperative and safe highway merging by providing reference speeds to drivers, and the cloud-aided active suspension of [7], which uses road preview of a cloud-based DT to update controller parameters and improve ride comfort remotely. These approaches enable advanced features via over-the-air updates rather than directly controlling the vehicle, aligning with the software-defined vehicle concept [8]. Conversely, direct control of connected and automated road vehicles for tasks such as steering control for lane-keeping [9] and emergency braking for hidden pedestrians in [10] demonstrates the feasibility of cloud-based control, but highlights stability concerns due to feedback delays introduced by network latencies [11].

The second approach, termed twin-in-the-loop, which was recently proposed [12], avoids network latencies by integrating a high-fidelity vehicle twin directly into the onboard control loop. The goal is to reduce end-of-line controller tuning requirements by reusing existing high-fidelity models from the product development stage. The twin-in-the-loop approach enhances controller performance for tasks such as braking [12] or state estimation [13], but comes at the cost of higher onboard computational demand, limiting the fidelity of the DT to only the vehicle twin and neglecting environment twins.

A central trade-off currently limits the application of DTs in vehicle dynamics control. On the one hand, cloud-based DTs provide a holistic environmental view with real-time road conditions but face stability issues in active control due to network latencies. On the other hand, onboard twins are stable but are limited by onboard computational resources. This trade-off defines a significant research gap: the potential of a holistic DT architecture to enhance vehicle dynamics control by integrating cloud-based information and offloading control functions to the cloud remains largely unexplored.

This article addresses this gap and examines how existing vehicle dynamics control functions, such as lateral stability, suspension, and powertrain control, could benefit from a holistic traffic DT. The paper advances the discourse on this topic by focusing on key considerations, such as DT model fidelity, data integration, and validation and verification, while exploring the inherent advantages and challenges of prospective DT services and cloud-based control.

To provide a tangible example, a use case for lateral vehicle stability is presented. This case features a scenario in which a demonstrator vehicle encounters varying road

surfaces and friction potentials, potentially approaching the limits of vehicle stability. A virtual representation of the environment and the vehicle is available in a cloud-based DT, which exchanges data with the vehicle over a public 4G network. The potential for DT services and cloud-control is experimentally demonstrated for two chassis control functions: Adaptive Cruise Control (ACC) and Torque Vectoring (TV).

The ACC experiments investigate how previewed road conditions, such as friction potential and curvature, facilitate safe speed adjustments and prevent loss of stability. The TV experiments investigate how proactive adjustments to the drive torque distribution support vehicle stability and handling for a human driver facing a potential loss of stability. Various configurations are explored, ranging from the DT acting as a control advisor to directly controlling the vehicle. The feasibility of cloud-based control for time-critical functions is studied, with a focus on communication latency under ideal conditions, by implementing parts or all of the ACC and TV algorithms in the cloud. Scalability and performance in large-scale deployments and under adverse network conditions are beyond the scope of this initial feasibility study.

The remainder of the paper is as follows: Section II discusses DT modelling fidelity, data integration, validation and verification, and prospective DT services for DT-enhanced vehicle dynamics control. Section III introduces the use case, separated into the DT framework in Sec. III-A, ACC and TV algorithms in Sec. III-B. Section IV presents the experimental results, followed by a discussion about open challenges in Section V. Section VI concludes the paper.

## II. DIGITAL TWINS FOR VEHICLE DYNAMICS CONTROL

While no universal definition exists, a DT is defined here as a dynamic, virtual replica of the physical world. Grieves' original DT concept comprises three dimensions: the physical twin, the virtual twin, and their connection [14]. The physical twin consists of various twin instances collectively forming a twin aggregate. These instances include the vehicle, the environment with traffic and road, and the driver. Virtual twin construction is more intricate, dictated by the required abstraction, accuracy, and specific use case.

The three-dimensional DT concept was extended to five in [15], integrating services and data. This framework makes data fundamental to DT creation. Services utilise information from other entities (physical twin, virtual twin, data) to enable or enhance features. Therefore, an initial discussion on information aggregation and virtual twin modelling is essential to discuss potential DT benefits and services for vehicle dynamics control.

### A. VIRTUAL VEHICLE DYNAMICS TWIN

Extensive research in vehicle dynamics provides a foundation for modelling individual DT instances, including the vehicle [16], driver [17], and road/environment [18].

Although predominantly physics-based, the field increasingly incorporates data-driven techniques, such as machine and deep learning, for applications like vehicle motion prediction [19]. The appropriate complexity of the virtual twin is a central consideration. This section examines the construction of the virtual twin from the perspective of physics-based vehicle modelling, focusing on model fidelity, validation and verification, and data integration.

### 1) MODEL FIDELITY

The notion of an all-encompassing multidisciplinary and multiphysics DT, capable of replicating reality with high fidelity, is a prevailing concept within the DT research field. The realisation of such a comprehensive digital representation, designed to evolve throughout a vehicle's operational lifespan, constitutes sophisticated models, such as four-wheel or multibody vehicle models, to capture all motion directions [20]. Furthermore, considerable tyre modelling is required, as it establishes the primary physical connection between the environment twin and the vehicle twin, as well as aerodynamic modelling for environmental influences like crosswinds [21]. The principal appeal of this approach lies in the model's inherent high-fidelity, which facilitates both the current support and the enablement of future services and applications, including those not yet conceived or thoroughly planned. Moreover, it allows the model to function as a "virtual sensor" or "soft sensor" in scenarios where real-world measurements are technically infeasible [1]. This conceptualisation aligns with a *top-down approach*, wherein the model's design enables subsidiary services rather than the reverse.

Although high-fidelity models provide a holistic system view, the widespread use of simpler, application-specific models reduces modelling effort and computational demands, especially in chassis control [3]. Kinematic models (e.g., point descriptions, kinematic two-wheel models) provide fundamental position and velocity information, primarily applied in traffic modelling. Quasi-static models (e.g., GG diagrams, handling diagrams) offer crucial insights into vehicle operational limits and cornering behaviour, proving invaluable for stability control applications. Simple dynamic models are employed to capture distinct motion directions: longitudinal models (e.g., the point mass model) used for speed control; lateral models (e.g., the dynamic two-wheel model) describe lateral and yaw motion, essential for path tracking tasks. Attitude models (e.g., quarter-car, half-car) capture vertical vehicle motion, which is crucial for ride comfort control. These specialised models facilitate the construction of a holistic DT through a *bottom-up approach*, integrating simpler models to capture the whole motion envelope. Here, services dictate the model fidelity. While this approach reduces modelling overhead, it risks insufficient DT fidelity for unforeseen future functionalities. Crucially, a DT's definition does not imply high complexity.

### 2) VALIDATION AND VERIFICATION (V&V)

V&V are crucial for ensuring confidence in and reliability of a DT. A key challenge is that vehicle parameters and characteristics change throughout the lifespan due to factors such as evolving tyre compounds, damper wear, or payload variations. This makes validation challenging and requires approaches that not only estimate parameter changes using traditional methods but also develop new data-driven techniques that utilise novel data sources, such as the fleet. Thus, V&V is an ongoing process rather than a single event at the development stage. V&V present greater challenges for top-down modelling than for bottom-up approaches.

The verification of a model following a top-down approach for general applicability is inherently more challenging than that of a bottom-up model, as it lacks the narrow, predefined specifications of a specific service and must cope with requirements that may change throughout the DT's lifespan.

Analogously, validating a top-down model is challenging because its accuracy is harder to quantify without a specific use case. Furthermore, validating a high-fidelity model can be difficult due to the difficulty or infeasibility of measuring certain system states, such as damper velocities. Although reusing previously validated models from vehicle development, as proposed by the twin-in-the-loop paradigm in [12], is a beneficial starting point, it does not eliminate the need for continuous V&V to account for in-service changes.

### 3) DATA INTEGRATION

An advantage of the DT paradigm over traditional model-based systems stems from the extensive availability of data and the interconnection between twin instances. Therefore, a rigorous *data integration* strategy is essential for managing information from diverse sources, such as the vehicle, its environment, and the fleet.

An aspect of data integration is distinguishing between static and dynamic data types [1]. Static data includes fixed vehicle properties, such as wheelbase, which are defined at the development stage. Dynamic data, however, changes with wear or operating conditions; examples include tyre characteristics, vehicle mass and centre of gravity location. Since direct and real-time measurement of dynamic data is often economically impractical or infeasible, continuous estimation is essential for maintaining the DT's fidelity. To this end, vehicle dynamics research has long relied on estimation methods. The traditional bottom-up approach uses specialised models and Kalman Filters for state and parameter estimation [22]. Recent top-down approaches, such as twin-in-the-loop observers, utilise high-fidelity vehicle models for more comprehensive, combined estimation [13].

However, the true paradigm shift offered by traffic DTs lies in their ability to replace specific onboard estimations entirely. By integrating vehicle data with global information from infrastructure, ultra-high-definition maps, or preceding vehicles, the DT provides predictive insights such as road banking, inclination, and road friction potential, effectively

eliminating the need for specific onboard estimation tasks. This goes beyond simply relocating conventional Kalman filtering to the cloud: the DT leverages shared, predictive information across vehicles and infrastructure to extend the spatial and temporal horizon of estimation.

While integrating environmental data into the vehicle twin is relatively straightforward, incorporating data from a heterogeneous vehicle fleet is challenging. Variability in vehicle types and sensors requires advanced processing to extract meaningful information, particularly for metadata that reflects critical driving events, such as skidding or emergency manoeuvres. Data cleaning, clustering, and mining techniques are therefore essential, and point towards advanced methods such as machine learning and deep learning. In particular, distributed approaches such as fleet learning [23] and federated learning [24] enable continuous model improvement across the fleet, providing estimation capabilities that surpass those of conventional onboard filtering.

## B. SERVICES FOR PROACTIVE VEHICLE DYNAMICS CONTROL

An advantage of a traffic DT is its ability to enable proactive vehicle dynamics control by anticipating or predicting upcoming critical driving conditions and adapting vehicle dynamics controllers accordingly to mitigate potentially adverse consequences. Proactive control relies on contextual awareness that overcomes onboard sensors' line-of-sight and range limitations, which creates opportunities for novel DT services to enhance chassis control systems [3].

A holistic traffic DT enables proactive safety responses, predicting potential collisions where standard Automatic Emergency Braking (AEB) systems might fail. The authors of [10] demonstrated this by initiating AEB remotely for occluded pedestrians based on traffic DT data. Integrating a friction potential map from the environment twin with the vehicle twin's known longitudinal dynamics further allows for optimising the AEB response. If braking is insufficient to avoid a collision, an emergency evasive manoeuvre may be initiated by augmenting or overriding driver steering inputs. This manoeuvre relies on a comprehensive understanding of the vehicle's lateral dynamics and environment to plan a safe trajectory while ensuring vehicle stability.

Proactively reconfiguring the vehicle's handling behaviour can enhance the execution of critical manoeuvres. This approach moves beyond simply making reactive systems, such as electronic stability control, more aggressive, as demonstrated using road topology data [25]. Temporarily modifying the vehicle's handling, rather than just adjusting the intervention, becomes possible. For example, a TV system can alter vehicle behaviour towards agility or stability by applying differential wheel torques. This capability enables proactive adaptation of the vehicle's handling: (1) in known upcoming events such as an AEB scenario, where braking alone cannot prevent a collision, the system can adjust

handling to be more agile via TV to support an evasive manoeuvre, and (2) in anticipated high-risk situations, such as when approaching dynamic limits on low-friction surfaces, it can proactively enhance stability by modifying the handling behaviour towards more understeer. Likewise, a steer-by-wire system could increase its steering ratio to improve the vehicle's responsiveness.

A key opportunity for the DT in vehicle handling lies in personalising the vehicle's response to the individual driver, dependent on upcoming road conditions, traffic and, importantly, the driver's skills. Achieving this capability requires a "driver twin" to learn and model individual driver behaviour [26]. Ultimately, the driver twin would inform the optimal TV or steer-by-wire strategy, creating a vehicle that is not only safer but also dynamically tailored to its driver.

These proactive adaptations extend to longitudinal motion control. Current ACC systems are already proactive, using static data such as road topology for speed adaptation [27]. A DT of the traffic adds a layer of dynamic awareness by integrating real-time traffic information, as shown for highway merging in [6], traffic flow optimisation in intelligent intersections in [2], or by enabling cooperative platooning in [28]. The DT's capabilities are extended by integrating real-time road conditions. By considering the optimal speed profile for road topology and friction potential, the system can proactively manage lateral vehicle stability by reducing vehicle speed, which is crucial in hazardous conditions like black ice while cornering.

Predictive information on road conditions benefits ride comfort control. Active suspension systems can enhance comfort by considering upcoming road unevenness from DT data; see [7]. As ride comfort highly depends on the speed at which an obstacle is passed [29], a detailed environment twin enables ACC to adapt speed proactively for both static obstacles, such as crosswalks, and temporary ones, like potholes. To improve comfort and traction, tyre pressure control systems, which possess slow dynamics, can be commanded proactively to adapt to upcoming road conditions.

Leveraging predictive information from the traffic flow increases powertrain efficiency. By considering traffic and route data, a powertrain controller can optimise its configuration, for instance, by decoupling a less-efficient motor or axle to reduce rotational inertia and operate the remaining motors at their peak efficiency, or an optimal speed profile incorporating extended lift-and-coast periods can be determined.

Predictive data from real-time weather services enables the vehicle to prepare for disturbances such as crosswinds. To mitigate lateral displacement and assist the driver, the system could proactively adjust a suspension, control active anti-roll bars, or increase the stiffness of a steer-by-wire system.

These examples illustrate that a holistic traffic DT is a versatile enabler for enhanced vehicle dynamics control, contributing via three primary services: providing enhanced vehicle models by integrating data sources such as vehicle



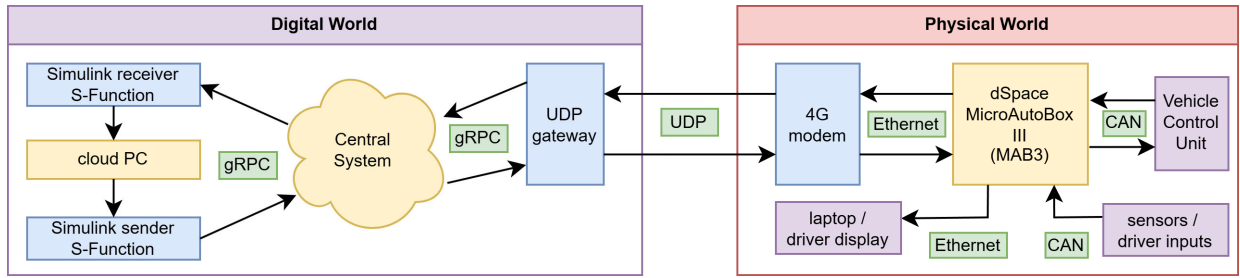


**FIGURE 2.** Used V2C architecture with the digital world (cloud-based) and the physical world (in-vehicle hardware). Communication between both worlds occurs over a 4G network. The diagram is colour-coded: computing nodes (yellow), gateways (blue), auxiliary nodes (purple), and communication protocols (green).

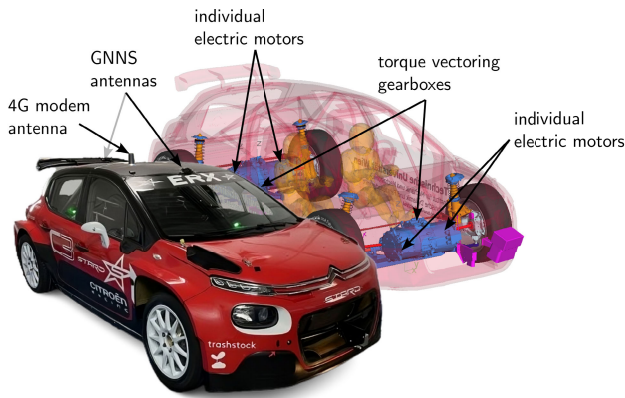


**FIGURE 3.** Demonstrator vehicle with its key systems. Individual electric motors and TV gearboxes enable differential torque control between the left and right sides. Antennas for GNSS and 4G communication are marked.

wheel. The core of the vehicle’s control system is a dSpace MicroAutoBox III (MAB3) rapid control prototyping unit; see Fig. 2. The MAB3 receives data from a suite of sensors connected via CAN bus, including a high-precision GNSS+IMU (OxTS RT3102) and driver input sensors. The MAB3 commands a vehicle control unit for actuation at 100 Hz, which controls the four electric motors. External communication is handled by a consumer-grade 4G modem connected to the MAB3 via Ethernet, with a laptop used for data visualisation, driver feedback and recording.

2) DIGITAL WORLD

The digital world in Fig. 2 is built around the Central System [4] that functions as a hub, managing data storage and facilitating communication between services via gRPC [31]. These services include a visualisation tool, which renders a 3D model of the vehicle and road, and a UDP gateway that handles communication with the physical vehicle. A key component is the cloud PC, a consumer-grade laptop running Ubuntu 22.04 and MATLAB Simulink R2024b, which sends data to the Central System via a custom S-Function at 100 Hz.

The cloud PC is central to the control architecture. It runs the control functions – detailed later – in various modes: advisory control, partial control, or complete cloud control.

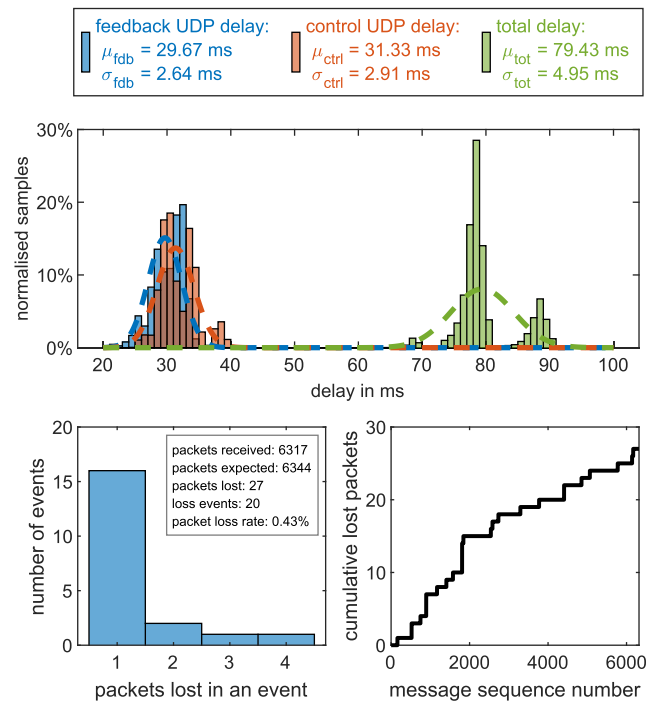


**FIGURE 4.** Packet delays are measured by synchronising the cloud PC, MAB3, and Central System via NTP. The message sequence number attached to each packet identifies packet losses.

It hosts the system’s two main twins. The environment twin consists of a pre-built map with navigation path and friction potential data. The friction potential map was derived from offline surface characterisation. The vehicle position in the environment twin is continuously updated using the transmitted GNSS data. The vehicle twin, a four-wheel planar vehicle model [32], utilises information from the environment twin and transmitted vehicle state data to assess lateral vehicle stability.

3) V2C COMMUNICATION

Communication between the digital and physical worlds is established over a 4G network using UDP [33], exchanging data at 100 Hz. The data exchange consists of a feedback message and a control message, both approximately 150 bytes. The feedback message sent from the vehicle to

the cloud contains vehicle state information (position, speed, etc.), driver inputs, and metadata. The control message sent from the cloud to the vehicle contains actuator commands, advisory settings, road data, and metadata.

To ensure data integrity and consistent timing, all computing nodes synchronise to a common time server via the NTP [34]. A custom NTP blockset was developed for the MAB3 unit, as it does not feature a native implementation. The 4G communication link underwent evaluation in a test with roughly 6300 samples to estimate delay and analyse packet loss between the digital and physical worlds. The Central System was located in Budapest, Hungary, while the cloud PC and the vehicle were at ZalaZONE, an air distance of roughly 180 km.

The UDP delays, shown in Fig. 4 in the top graph, exhibit a normal distribution with means of  $\mu_{fdb} = 29.67$  ms for feedback (blue) and  $\mu_{ctrl} = 31.33$  ms for control (orange) messages. The total delay (green) is  $\mu_{tot} = 79.43$  ms. The difference of approximately 20 ms between  $\mu_{tot}$  and  $\mu_{fdb} + \mu_{ctrl}$  is primarily attributed to gRPC delays. The bottom graphs in Fig. 4 show packet losses. Across 20 discrete events, 27 packets were lost, resulting in a loss rate of 0.43 %. Most were single-packet losses, with a maximum consecutive loss of four packets observed.

This analysis highlights the importance of monitoring real-time delays and incorporating fallback strategies, such as complete onboard control, in the event of prolonged communication failure. However, subsequent experiments did not employ such an alternative strategy.

## B. CONTROL METHODS

For controller synthesis, a top-down modelling approach is used, starting from a validated high-fidelity multibody model of the demonstrator vehicle; shown in Fig. 3. This model enables the parametrisation of a four-wheel planar vehicle model, which includes a wheel load model based on longitudinal  $a_x$  and lateral  $a_y$  accelerations [32]. This simpler model satisfies the fidelity requirements of ACC and TV. A global representation of the vehicle's limits, such as a GG diagram, can be extracted for ACC. The model provides appropriate information on how individual motor torques influence vehicle dynamics for TV.

### 1) ACC

Enhancing ACC with navigation data is a common method for improving comfort, efficiency and safety. However, it relies on static maps without knowledge of upcoming road conditions and simple vehicle limit approximations, neglecting the combined effects of acceleration and braking [27]. To address this latter limitation, this work employs a GG diagram computed by formulating a Nonlinear Programming (NLP) problem with *CasADi* [35]. The NLP assumes quasi-steady-state conditions for the vehicle model and a given friction coefficient  $\mu$  and uses *Ipopt* [36] as a solver, with further details on the computation available in [37]. The

NLP yields the GG diagram in polar coordinates, defined by the angle  $\alpha = \tan^{-1}(a_x/a_y)$  and the corresponding radii  $a_{GG} = f_{GG}(\alpha, \mu)$ .

A simple approach to limit vehicle speed  $V$  in a corner involves applying a steady-state limit  $V_{lim}^{ss}$ :

$$V_{lim}^{ss}(\rho, \mu, \eta) = \sqrt{\frac{\eta f_{GG}(\alpha = 0, \mu)}{|\rho|}}, \quad (1)$$

where  $\rho$  denotes road curvature and  $\eta$  is a safety factor. Although this method reduces vehicle speed enough to maintain stability for a low-friction corner, it fails to account for the combined effects of braking and cornering, which can still lead to a loss of lateral stability.

A more advanced solution involves proactive speed planning for ACC, generating a speed profile  $\mathbf{V}$  by considering upcoming road conditions and the whole GG diagram. This formulation treats the speed planning as a reference speed tracking problem and defines its solution over a fixed preview length of  $N$  steps with step length  $\Delta s$  as follows:

$$\min_{\mathbf{V} \in \mathbb{R}^N, s_{GG} \in \mathbb{R}} q_s s_{GG}^2 + \sum_{i=1}^N q_{a_x} a_{x,i}^2 + q_V (V_{ref} - V_i)^2 \quad (2a)$$

$$\text{subject to } a_{x,i}^2 + a_{y,i}^2 \leq (a_{lim,i} + s_{GG})^2, \quad (2b)$$

$$0 \leq V_i \leq V_{max}, \quad (2c)$$

$$a_{x,min} \leq a_{x,i} \leq a_{x,max}, \quad (2d)$$

$$a_{x,i} = \frac{1}{2\Delta s} (V_i^2 - V_{i-1}^2), \quad (2e)$$

$$a_{y,i} = \rho_i V_i^2, \quad (2f)$$

$$V_0 = V_{init}. \quad (2g)$$

Here, the terms  $q_V$ ,  $q_{a_x}$ , and  $q_s$  are tuning weights to balance reference speed tracking, longitudinal acceleration, and adhering to the vehicle's handling limits, respectively. Adding the slack variable  $s_{GG}$  improves feasibility. The ACC speed is set by  $V_{ref}$ . The problem is constrained by speed limit  $V_{max}$ , longitudinal acceleration limits  $a_{x,min}$  and  $a_{x,max}$ , and the combined acceleration limit from the GG diagram  $a_{lim,i} = \eta f_{GG}(\hat{\alpha}_i, \mu_i)$ . The GG angle  $\hat{\alpha}_i$  and initial speed  $V_{init}$  stem from the previous execution of the planner. For real-time applicability, the planner uses a Sequential Quadratic Programming (SQP) method that employs the *OSQP* solver [38]. A P-controller tracks the planned speed profile  $\mathbf{V}$  onboard.

### 2) TV

TV actively influences vehicle lateral dynamics for stabilisation and handling modification. For stabilisation, TV operates similarly to electronic stability control by braking individual wheels, but with the added ability to apply drive torques for more comprehensive intervention. For handling modification, TV allows shaping the vehicle's quasi-steady-state cornering response by directly influencing its steering characteristic.

The steering characteristic  $\delta_{dyn}(a_y)$  is described by the dynamic steering-wheel angle  $\delta_{dyn} = \delta - l\rho$  as a function

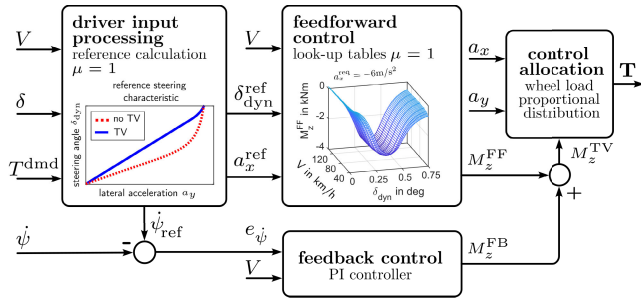


**FIGURE 5.** TV architecture for a given friction coefficient  $\mu$  and steering characteristic  $\delta_{dyn}(a_y)$ . The TV yaw moment  $M_z^{TV}$  combines a feedforward term  $M_z^{FF}$  from look-up tables with a feedback term  $M_z^{FB}$  from a PI controller. The system allocates this moment to motor torques  $\mathbf{T}$  based on wheel loads.

of lateral acceleration  $a_y$  [21]. Here,  $\delta$  is the actual steering angle, and  $l$  is the vehicle’s wheelbase. A typical passenger vehicle exhibits a near-linear relationship of  $\delta_{dyn}(a_y)$  up to approximately 50% of maximal feasible lateral acceleration  $a_y^{max}$ . In this region, the steering angle gradient  $K_\delta = \partial\delta_{dyn}/\partial a_y$  remains nearly constant. Beyond this linear range, the characteristic becomes nonlinear as tyres saturate.

The steering characteristic defines a vehicle as understeering ( $K_\delta > 0$ ), neutralsteering ( $K_\delta = 0$ ), or oversteering ( $K_\delta < 0$ ) [21]. Understeering is generally considered stable and predictable, while neutral and oversteering behaviours can challenge inexperienced drivers. Actively shaping the steering characteristic allows the vehicle to tailor its handling to a driver’s preference or skill level and dynamically adapt to upcoming road conditions, aiding the driver in hazardous situations. TV can shape this characteristic by applying an additional yaw moment  $M_z^{TV}$ . With this additional yaw moment, the system can impose a specific steering angle gradient, extend the linear range, or increase the maximum feasible lateral acceleration  $a_y^{max}$ . Thus, the TV system can be proactively reconfigured based on information from a traffic DT.

The employed TV control, based on methods from [39] and [40], follows the architecture shown in Fig. 5. The upcoming paragraphs provide a brief overview; refer to the cited publications for additional information.

First, reference values based on steering input  $\delta$ , torque demand  $T^{dmd}$ , derived from the throttle pedal position, and vehicle speed  $V$  are calculated. These are the yaw rate  $\dot{\psi}_{ref}$  and the dynamic steering angle  $\delta_{dyn}^{ref}$ , which result from a demanded steering characteristic  $\delta_{dyn}(a_y)$ , and the longitudinal acceleration  $a_x^{ref}$ .

Second, a corrective yaw moment  $M_z^{TV}$  is computed as the sum of feedforward (FF) and feedback (FB) yaw moments:

$$M_z^{TV} = M_z^{FF} + M_z^{FB}. \quad (3)$$

A look-up table provides the feedforward term  $M_z^{FF}$ . It is pre-computed by solving an NLP problem, formulated in *CasADi* and solved with *Ipopt*, that defines the optimal yaw moment to achieve the given steering characteristic  $\delta_{dyn}(a_y)$  [39].

The NLP uses the four-wheel planar vehicle model in quasi-steady-state conditions and depends on vehicle speed  $V$ , dynamic steering angle  $\delta_{dyn}^{ref}$ , longitudinal acceleration  $a_x^{ref}$ , and friction coefficient  $\mu$ . Consequently, the table is high-dimensional, rendering it both memory-intensive and computationally demanding to recompute. The feedback term  $M_z^{FB}$  is the output of a PI controller that minimises the error between the reference and measured yaw rates  $e_{\dot{\psi}} = \dot{\psi}_{ref} - \dot{\psi}$  [40].

Third, the total yaw moment  $M_z^{TV}$  is allocated to the individual motor torques  $\mathbf{T}$  using a strategy that distributes the yaw moment based on the vertical force on each wheel [40].

#### IV. EXPERIMENTS

The control methods, ACC and TV, from Sec. III-B are tested in various configurations, comparing performance with and without DT assistance across the three cloud-based control modes: advisory, partial, and complete cloud control.

##### A. ACC EXPERIMENTS

For the ACC experiments, the cloud provides advisory or reference vehicle speeds based on information from the environment twin and vehicle twin (handling envelope, vehicle position). The three control modes are:

- **Advisory Cloud Control:** The cloud calculates a speed limit  $V_{lim}$  and sends it to the driver display. The driver controls the vehicle speed  $V$ . The display provides a visual warning if the driver exceeds  $V_{lim}$ ; see Fig. 6. The speed limit  $V_{lim}$  is the minimum of the reference speed  $V_{ref}$  and the lateral limit speed  $V_{lat}$ . The lateral limit speed  $V_{lat}$  is the lowest feasible steady-state speed limit  $V_{lim}^{ss}$  within a preview distance  $s_{prev}$  from the current vehicle position  $s$ :

$$V_{lat}(\eta) = \min_{\hat{s} \in [s, s+s_{prev}]} V_{lim}^{ss}(\rho(\hat{s}), \mu(\hat{s}), \eta) \quad (4)$$

- **Partial Cloud Control:** The cloud handles high-level planning using the ACC planner from (2), sending the first value of the speed profile  $\mathbf{V}$  in a receding horizon manner to the vehicle. An onboard P-controller performs speed tracking.
- **Complete Cloud Control:** The cloud performs high-level planning and low-level tracking and sends the final motor torque commands to the vehicle.

Table 1 lists the ACC parameters for the experiments.

Fig. 7 compares the resulting vehicle trajectory and speed profile of two advisory cloud control experiments: a baseline without driver warning (magenta) and an experiment with visual warning enabled (blue). The left plot shows the vehicle’s GNSS trajectories, with a zoom of the critical section near the 225 m mark. The right plot shows the vehicle speeds against the speed limit  $V_{lim}$ , the lateral limit speed  $V_{lat}(\eta = 1)$  calculated without safety margin, and the reference speed  $V_{ref}$ .

A steep descent of the road towards the low-friction area made speed control challenging for the driver, resulting in

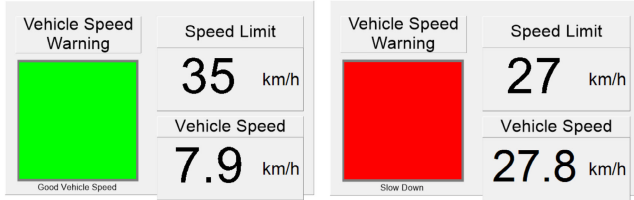


**FIGURE 6.** The vehicle speed monitoring system displays a safe condition (green, left) or a warning (red and alert, right) when the driver exceeds the speed limit  $V_{lim}$ , which is transmitted via 4G to the vehicle.

**TABLE 1.** Parameters used in the ACC experiments.

Name	Value	Unit	Description
$s_{prev}$	50	m	preview length
$N$	20	-	number of steps in planner
$\Delta s$	2.5	m	step length in planner
$a_{x,max}$	2.5	$m/s^2$	maximum allowed acceleration
$a_{x,min}$	-2.5	$m/s^2$	minimum allowed acceleration
$V_{max}$	35	km/h	maximum allowed vehicle speed
$V_{ref}$	35	km/h	reference speed in planner
$\eta$	0.9	-	safety factor
$g$	9.81	$m/s^2$	acceleration of gravity
$q_V$	$1/V_{ref}^2$	$(m/s)^{-2}$	reference speed tracking weight
$q_{a_x}$	$0.5/g^2$	$(m/s^2)^{-2}$	longitudinal acceleration weight
$q_s$	$200N/g^2$	$(m/s^2)^{-2}$	GG diagram slack weight

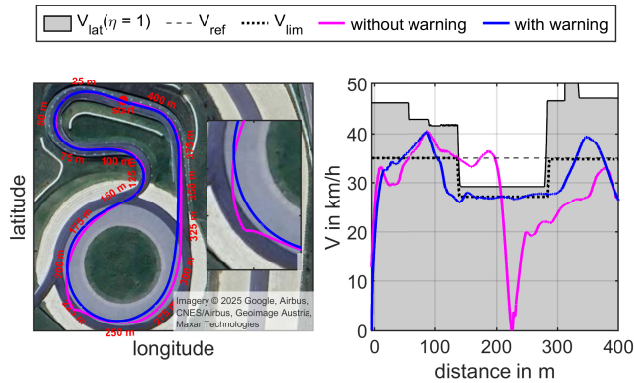


**FIGURE 7.** Advisory cloud control with and without driver warning. Left plot: path without driver warning (magenta) and with driver warning (blue). Right plot: vehicle speeds against speed limit  $V_{lim}$  (dotted), lateral limit speed  $V_{lat}(\eta = 1)$  without safety margin (shaded area), and reference speed  $V_{ref}$  (dashed).

the overshoot at 100 m. Without driver warning, the driver attempted to maintain  $V_{ref} = 35$  km/h into the low-friction corner. This entry speed was excessive, resulting in a loss of stability at the 200 m mark, which caused the vehicle to deviate from its intended path. With driver warning, the driver followed the speed limit  $V_{lim}$  and navigated the corner without loss of stability.

Fig. 8 compares the partial (magenta) and complete (blue) ACC cloud control. The left plot shows the vehicle speeds against the ACC planner speed, the speed limit  $V_{lim}$  from the advisory cloud control, and the reference speed  $V_{ref}$ . The right plot shows the resulting GG diagram for the partial cloud control experiment, segmented into high- and low-friction regions.

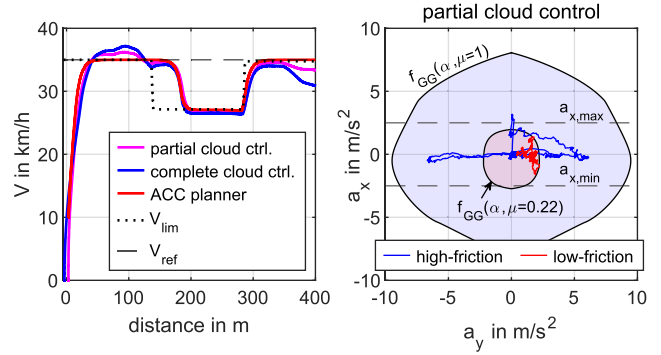


**FIGURE 8.** Partial (magenta) and complete (blue) ACC cloud control results. Left plot: vehicle speeds against speed limit  $V_{lim}$  (dotted), ACC planner speed (red), and reference speed  $V_{ref}$  (dashed). Right plot: GG diagram for partial cloud control separated into high-friction (blue) and low-friction (red) segments.

The tracking of the ACC planner speed is accurate in the low-friction segment between 150 m and 300 m for both experiments. Compared to the advisory cloud control, braking occurs later, as the ACC planner utilises the full GG envelope, while the advisory cloud control is constrained by the steady-state limit  $V_{lim}^{ss}$ . The GG plot highlights that the vehicle operates near the boundary of  $f_{GG}(\alpha, \mu = 0.22)$ . Given the small communication latencies shown in Fig. 4, the performance of the complete cloud control is similar to that of the partial cloud control case. Minor deviations appear around 100 m (from a steep descent of the road) and 400 m (from a steep incline), which result from different P-controller parameters but do not affect the critical low-friction section.

### B. TV EXPERIMENTS

For the TV experiments, four sets of look-up tables were computed offline. These sets correspond to combinations of two friction coefficients  $\mu$  and two steering characteristics  $\delta_{dyn}(a_y)$ . The latter are distinguished primarily by their understeer gradients  $K_\delta$ : the passive vehicle gradient  $K_\delta^{psv}$  and a selected, larger understeering gradient  $K_\delta^{us}$ . The experiments include three modes again:

- Advisory Cloud Control: The cloud provides high-level advice to the onboard TV controller by selecting the most appropriate steering characteristic  $\delta_{dyn}(a_y)$  for the upcoming conditions. The selection is based on the friction coefficient  $\mu$  and a lateral stability index  $I_{lat}$  which quantifies how close the vehicle state is to the handling limit over a future time horizon  $T_{prev}$ :

$$I_{lat}(\eta) = \max_{\hat{s} \in [s, s+VT_{prev}]} \frac{a_{y,prev}^{ss}}{a_{y,lim}^{ss}}. \quad (5)$$

Here,  $a_{y,prev}^{ss}$  is computed with  $V^2 |\rho(\hat{s})|$  assuming constant vehicle speed  $V$ , and  $a_{y,lim}^{ss}$  is given by  $\eta f_{GG}(\alpha = 0, \mu(\hat{s}))$ . Using a hysteresis-based switching logic, the TV set switches  $K_\delta^{psv}$  to  $K_\delta^{us}$  when  $I_{lat}$  exceeds a switch point  $I_{SP}$ , and back again when it drops below a reset point  $I_{RP}$ .

TABLE 2. Additional parameters used in the TV experiments.

Name	Value	Unit	Description
$\mu$	{0.22, 1}	-	friction potential levels in TV sets
$K_{\delta}^{PSV}$	0.057	s <sup>2</sup> deg/m	passive steering angle gradient
$K_{\delta}^{US}$	0.15	s <sup>2</sup> deg/m	larger understeering gradient
$T_{prev}$	1	s	preview time for $I_{lat}$
$I_{SP}$	0.9	-	switch point for $I_{lat}$
$I_{RP}$	0.6	-	reset point for $I_{lat}$

- Partial Cloud Control: This mode extends the advisory cloud control by offloading the driver input processing and feedforward control blocks of Fig. 5 to the cloud. The feedback controller and allocation logic remain onboard the vehicle.
- Complete Cloud Control: This mode executes the entire TV architecture in the cloud and transmits motor torque commands to the vehicle.

Table 2 lists the parameters for the TV experiments.

Fig. 9 compares the performance of five experiments: no TV (black), non-DT-enhanced TV with  $K_{\delta}^{PSV}$  (blue), and three levels of cloud involvement (advisory in magenta, partial in green, complete in red). The non-DT-enhanced TV case represents a non-communicating vehicle using TV with a fixed steering characteristic, whereas in the DT-enhanced cases, the steering characteristic is adjusted over 4G according to the proactive control strategy. Close to 225 m, a disturbance, unknown to the controller and DT, is manually triggered to destabilise the vehicle. This disturbance is a 120 Nm torque pulse applied to both rear motors for 0.1 s. The vehicle’s trajectory (top) and sideslip angle  $\beta$  (middle) reveal the response of the vehicle to the disturbance, while the feedforward  $M_z^{FF}$  and feedback  $M_z^{FB}$  yaw moments (bottom) show the controller’s internal states.

TV experiments were conducted with two driver types: a non-reacting (unskilled) driver and a countersteering (skilled) driver, who attempts to stabilise the vehicle. Even with countersteering, the vehicle is difficult or impossible to stabilise on the low-friction surface without TV. Fig. 9 shows the non-reacting, unskilled driver, characterised by constant steering and throttle inputs after the disturbance, isolating the effect of the DT-enabled proactive control strategy. Feedback controller gains were identical across all experiments.

Without TV (black, Fig. 9), the vehicle sideslip angle  $\beta$  increases significantly, causing the vehicle to lose considerably speed and ultimately to point in the opposite driving direction. The non-DT-enhanced TV (blue) stabilises the vehicle trajectory by limiting the sideslip angle  $\beta$  to  $-12$  deg. The recovery phase takes approximately 50 m or 6 s, meanwhile, it is difficult for a driver to control the vehicle. The feedforward term  $M_z^{FF}$  is small and relatively constant, as there is no proactive control and the control aim is the vehicle’s passive behaviour. The feedback term  $M_z^{FB}$  first applies a negative moment to counteract the skidding motion, reducing the vehicle sideslip angle  $\beta$  and the desired yaw rate  $\dot{\psi}$ . Subsequently, the controller applies a positive moment to

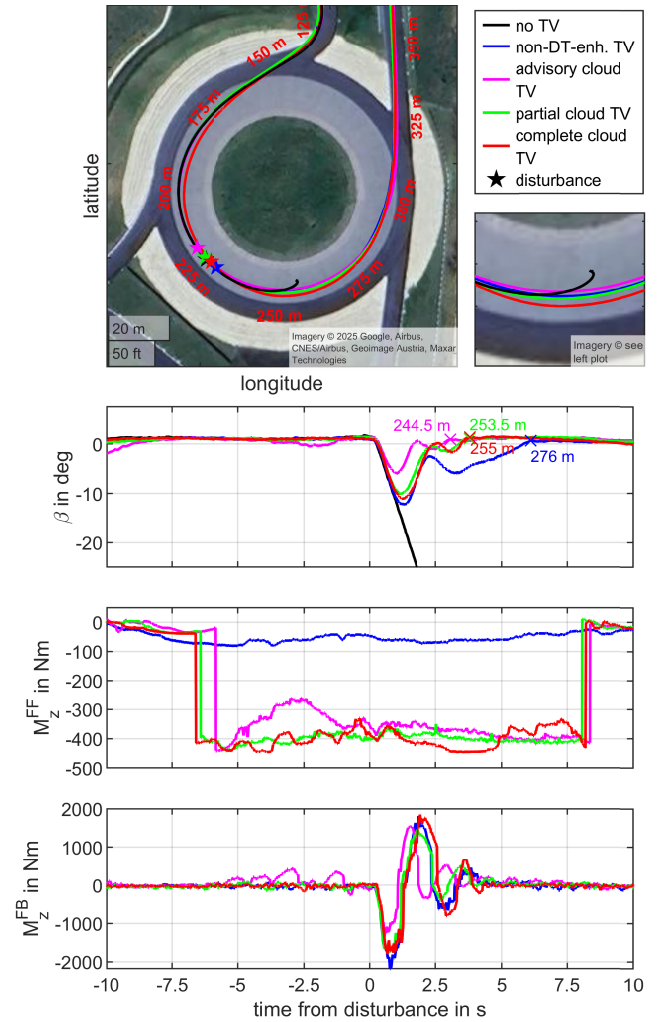


FIGURE 9. TV results for advisory (magenta), partial (green) and complete (red) cloud control with a disturbance at 225 m. Reference cases: no TV (black) and non-DT-enhanced TV (blue). Top row: vehicle’s trajectory. Second row: vehicle’s sideslip angle  $\beta$ . Bottom two rows: feedforward yaw moment  $M_z^{FF}$  and feedback yaw moment  $M_z^{FB}$  of TV controller.

turn the vehicle back into the corner, allowing the driver to maintain the intended path.

The vehicle stabilisation phase significantly shortens with the advisory cloud control (magenta, Fig. 9). The recovery distance and time are reduced by 50 % compared to the non-DT-enhanced case, to 20 m and 3 s respectively. This improvement results from the cloud, which proactively switches the TV set to a larger understeering characteristic. This characteristic results in a larger negative feedforward yaw moment  $M_z^{FF}$ , making the vehicle less prone to skidding. The feedback yaw moment  $M_z^{FB}$  behaviour remains similar.

Fig. 10 shows the control logic for TV set selection. Before the 200 m mark, the TV set switches to the low-friction steering gradient  $K_{\delta}^{PSV}$ . As the vehicle approaches the lateral limit behaviour, the stability index  $I_{lat}$  triggers a change to the larger understeering gradient  $K_{\delta}^{US}$  at 200 m, causing the distinct jump in the feedforward yaw moment  $M_z^{FF}$  seen in Fig. 9 at  $-6$  s.

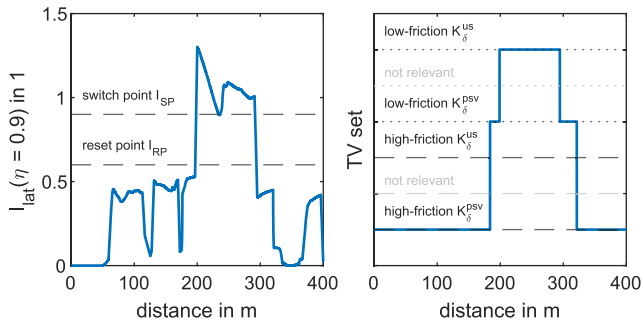


FIGURE 10. Lateral stability index  $I_{lat}$  and the resulting behaviour of the active TV set for the advisory cloud control experiment of Fig. 9.

The partial (green, Fig. 9) and complete (red, Fig. 9) cloud control cases perform similarly to the advisory cloud control case, with recovery distance and time reduced by 36 %, to 22 m and 3.8 s, respectively. The differences in peak vehicle sideslip angle  $\beta$  and recovery performance observed after the disturbance between the three DT-enhanced configurations are attributed to inaccuracies in manually triggering the disturbance, which resulted in slightly different friction potentials at the disturbance.

Experiments with the countersteering driver show a slightly smaller peak of the vehicle sideslip angle  $\beta$  after the disturbance, but similar reduction in recovery times and distance as in Fig. 9. Across 16 TV runs, including both driver types, DT-enhanced cases ( $n = 8$ ) showed a mean recovery time reduction of  $39.6 \% \pm 3.5 \%$  relative to non-DT-enhanced cases ( $n = 8$ ).

Although the total time delay  $\mu_{tot}$  of approximately 80 ms (Fig. 4) had a negligible impact on the performance, this result must be interpreted in light of the controlled environment. The experiments were carried out under ideal network conditions on a proving ground with minimal 4G traffic and no physical obstructions. In densely populated areas, the communication time delays could fluctuate and increase significantly, posing a greater challenge to closed-loop stability.

The destabilising effect of larger time delays is well documented in automotive feedback loops [11]. To investigate this issue, the total communication time delay  $\mu_{tot}$  was artificially enlarged using a delay block in the cloud PC. Fig. 11 shows results from four experiments with complete cloud control: the baseline 80 ms delay (black) and additional delays of +50 ms (blue), +100 ms (magenta), and +250 ms (green). The impact of larger delays on disturbance rejection is shown with the vehicle sideslip angle  $\beta$  (top) and the feedback yaw moment  $M_z^{FB}$  (bottom).

The results show a degradation in performance with increasing time delay. The +50 ms case slightly extends the recovery phase. At +100 ms, the system behaviour becomes oscillatory. The recovery phase extends significantly and is similar to the non-DT-enhanced case shown in Fig. 9. A delay of +250 ms pushes the system to its limits, causing feedback control saturation and a significant reduction in vehicle speed. The shorter recovery time observed in this

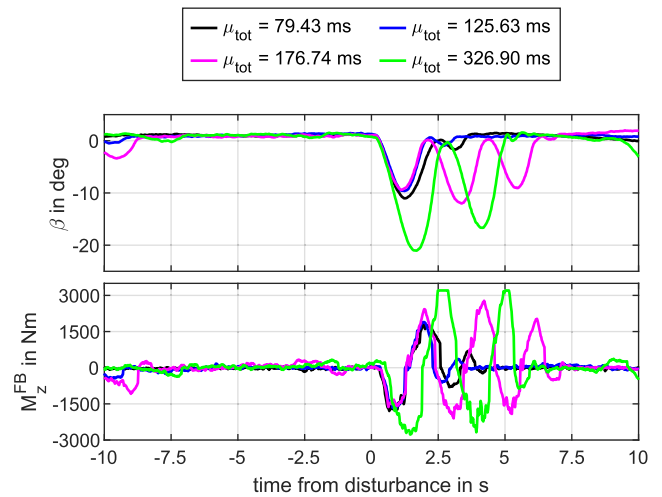


FIGURE 11. Complete cloud control TV experiments with increasing time delay  $\mu_{tot}$ . Experiments shown: baseline 80 ms delay (black) and additional delays of +50 ms (blue), +100 ms (magenta), and +250 ms (green). Top row: vehicle sideslip angle  $\beta$ . Bottom row: feedback yaw moment  $M_z^{FB}$  of TV controller.

case results from the reduced speed rather than improved system response. Additionally, the driver could subjectively perceive the larger communication time delays through a delayed throttle response.

## V. DISCUSSION

While the experiments investigated the potential of cloud-based DT for vehicle dynamics control, significant, unaddressed challenges remain to make this concept viable.

The simple vehicle and environment twins demonstrated potential, but maintaining their validity over time demands continuous model validation and parameter estimation. Model-to-reality mismatches can have safety-critical effects, such as overestimating friction potential or the vehicle’s GG diagram, leading to loss of stability. Further research into data integration methods, including machine and deep learning approaches such as fleet and federated learning, could reduce these mismatches through continuous refinement and validation.

Complete cloud control, as demonstrated in the TV use case, is vulnerable to large communication delays that can destabilise feedback loops and degrade controller performance. While the experiments were conducted under favourable conditions on a proving ground, other network-related issues, such as extended outages through tunnels or congestion in urban areas, pose similar stability risks and must be taken into account. Similarly, cybersecurity is a critical concern, as malicious packet injections could lead to hazardous control actions, especially in the case of complete cloud control. Advancing this first demonstration requires robust strategies with fallback mechanisms to handle large delays, dropouts, and temporary connectivity losses. Promising directions include adaptive control architectures that seamlessly switch between cloud and onboard modes by monitoring delays, model-based delay compensation,

and redundant communication links, such as 5G or Dedicated Short-Range Communication (DSRC), to enhance resilience [4], [10].

Considering more vehicles in the use case, the computational effort or scalability per vehicle may become relevant. Each control cycle, including the ACC optimisation, required approximately 2-5 ms on the cloud PC. For the TV use cases, computation time remained below 1 ms as only look-up tables were used. So when no server-side load balancing is considered, the computation time should scale linearly with the number of vehicles. Since this work is based on an existing V2C infrastructure, readers are referred to [4] for detailed analyses of load sharing and computational scalability.

Given these limitations, the most practical near-term application of the cloud-based paradigm lies in advisory or partial control, where the cloud assists onboard systems through computational offloading, predictive insights, or fleet-level knowledge. Such a hybrid approach combines the scalability and situational awareness of cloud computing with the reliability and safety of local control, providing a path toward increasing cloud involvement in chassis systems.

## VI. CONCLUSION

A holistic traffic Digital Twin (DT) is a versatile enabler for enhanced vehicle dynamics control. By integrating a vehicle twin of suitable fidelity with real-time environmental and traffic twins, its contributions fall into three services: providing enhanced vehicle models by integrating data sources such as vehicle fleets or infrastructure, providing enhanced contextual awareness for proactive strategies, and facilitating personalised vehicle dynamics control to assist the driver.

Integrating these services with a cloud architecture can reduce onboard hardware requirements by lowering computational and memory demands. This paper experimentally evaluates these concepts in a use case featuring proactive adjustments to Adaptive Cruise Control (ACC) and Torque Vectoring (TV) under low-friction conditions, aiming to maintain or improve stability and handling for a human driver.

For ACC, it was demonstrated that the approach ensures stability in low-friction sections by proactively informing a human driver about safe driving speeds, adjusting reference speeds for an onboard ACC, or executing the ACC entirely in the cloud. The system's effectiveness relies on knowledge of the vehicle's stability envelope, as depicted in a GG diagram. The cloud architecture provides the necessary computational power to update the vehicle twin and recompute this diagram over the vehicle's lifespan, thereby ensuring the validity of its safety-critical speed advisories.

For TV, it was demonstrated that proactive adjustments of the controller based on upcoming road conditions can assist a human driver in the event of vehicle destabilisation, reducing recovery distance and time by up to 50 % compared to non-DT-enhanced TV. Experiments demonstrated that executing parts or the entire TV architecture is feasible over 4G networks without notable performance degradation

compared to onboard control, enabling the offloading of memory-intensive look-up tables. These findings indicate that direct cloud-based control of vehicle yaw motion may be a suitable future application for assisting vehicles in critical scenarios. However, challenges remain that hinder the practical application of this use case, including robustness, cybersecurity, and latency of the communication link.

## ACKNOWLEDGMENT

The authors thank STARD for providing the test vehicle and support. Special thanks extend to Dr. András Rövid and Ádám Boronyák for their assistance with testing, support, and operation of the Central System.

## REFERENCES

- [1] M. Spiriyagin, J. Edelmann, F. Klinger, and C. Cole, "Vehicle system dynamics in digital twin studies in rail and road domains," *Vehicle Syst. Dyn.*, vol. 61, no. 7, pp. 1737–1786, Jul. 2023.
- [2] A. L. Gratzter, M. M. Broger, A. Schirrer, and S. Jakubek, "Two-layer MPC architecture for efficient mixed-integer-informed obstacle avoidance in real-time," *IEEE Trans. Intell. Transp. Syst.*, vol. 25, no. 10, pp. 13767–13784, Oct. 2024.
- [3] V. Mazzilli, S. De Pinto, L. Pascali, M. Contrino, F. Bottiglione, G. Mantriota, P. Gruber, and A. Sorniotti, "Integrated chassis control: Classification, analysis and future trends," *Annu. Rev. Control*, vol. 51, pp. 172–205, Jan. 2021.
- [4] V. Tihanyi, A. Rövid, V. Remeli, Z. Vincze, M. Csonthó, Z. Pethő, M. Szalai, B. Varga, A. Khalil, and Z. Szalay, "Towards cooperative perception services for ITS: Digital twin in the automotive edge cloud," *Energies*, vol. 14, no. 18, p. 5930, Sep. 2021.
- [5] S. Carney. (Dec. 2024). *Mcity Unveils Digital Twin, Making Its Physical AV Testing Facility Available for Free in the Virtual World*. [Online]. Available: <https://mcity.umich.edu/mcity-unveils-digital-twin-making-its-physical-av-testing-facility-available-for-free-in-the-virtual-world/>
- [6] Z. Wang, X. Liao, X. Zhao, K. Han, P. K. Tiwari, M. Barth, and G. Wu, "A digital twin paradigm: Vehicle-to-cloud based advanced driver assistance systems," in *Proc. IEEE 91st Veh. Technol. Conf. (VTC-Spring)*, May 2020, pp. 1–6.
- [7] X. Zheng, H. Zhang, H. Yan, F. Yang, Z. Wang, and L. Vlacic, "Active full-vehicle suspension control via cloud-aided adaptive backstepping approach," *IEEE Trans. Cybern.*, vol. 50, no. 7, pp. 3113–3124, Jul. 2020.
- [8] Z. Liu, W. Zhang, and F. Zhao, "Impact, challenges and prospect of software-defined vehicles," *Automot. Innov.*, vol. 5, no. 2, pp. 180–194, Apr. 2022.
- [9] S. Beregi, S. S. Avedisov, C. R. He, D. Takács, and G. Orosz, "Connectivity-based delay-tolerant control of automated vehicles: Theory and experiments," *IEEE Trans. Intell. Vehicles*, vol. 8, no. 1, pp. 275–289, Jan. 2023.
- [10] A. Rovid, V. Tihanyi, M. Csermi, M. Csontho, A. Domina, V. Remeli, Z. Vincze, M. Szanto, M. Szalai, S. Nagy, and Z. Szalay, "Digital twin and cloud based remote control of vehicles," in *Proc. IEEE Int. Conf. Mobility, Operations, Services Technol. (MOST)*, May 2024, pp. 154–167.
- [11] A. Bartfai, I. Voros, and D. Takacs, "Stability analysis of a digital hierarchical steering controller of autonomous vehicles with multiple time delays," *J. Vib. Control*, vol. 30, nos. 1–2, pp. 330–341, Jan. 2024.
- [12] F. Dettü, S. Formentin, and S. M. Savaresi, "The twin-in-the-loop approach for vehicle dynamics control," *IEEE/ASME Trans. Mechatronics*, vol. 29, no. 2, pp. 1217–1228, Apr. 2024.
- [13] F. Dettü, S. Formentin, and S. Matteo Savaresi, "Joint vehicle state and parameters estimation via twin-in-the-loop observers," *Vehicle Syst. Dyn.*, vol. 62, no. 9, pp. 2423–2449, Sep. 2024.
- [14] M. W. Grieves, "Digital twins: Past, present, and future," in *The Digital Twin*. Cham, Switzerland: Springer, 2023, pp. 97–121.
- [15] F. Tao, M. Zhang, and A. Y. C. Nee, "Chapter 3—five-dimension digital twin modeling and its key technologies," in *Digital Twin Driven Smart Manufacturing*. New York, NY, USA: Academic, Jan. 2020, ch. 3, pp. 63–81.
- [16] D. J. N. Limebeer and M. Massaro, *Dynamics and Optimal Control of Road Vehicles*. London, U.K.: Oxford Univ. Press, 2018.

- [17] M. Plöchl and J. Edelmann, "Driver models in automobile dynamics application," *Vehicle Syst. Dyn.*, vol. 45, nos. 7–8, pp. 699–741, Jul. 2007.
- [18] D. J. N. Limebeer and E. Warren, "A review of road models for vehicular control," *Vehicle Syst. Dyn.*, vol. 61, no. 6, pp. 1449–1475, Jun. 2023.
- [19] L. Hermansdorfer, R. Trauth, J. Betz, and M. Lienkamp, "End-to-end neural network for vehicle dynamics modeling," in *Proc. 6th IEEE Congr. Inf. Sci. Technol. (CiSt)*, Jun. 2020, pp. 407–412.
- [20] P. Lugner and M. Plöchl, "Modelling in vehicle dynamics of automobiles," *J. Appl. Math. Mech.*, vol. 84, no. 4, pp. 219–236, Apr. 2004.
- [21] H. B. Pacejka, *Tire and Vehicle Dynamics*. Warrendale, PA, USA: SAE, 2006.
- [22] M. Doumiati, A. Charara, A. Victorino, D. Lechner, and B. Dubuisson, *Vehicle Dynamics Estimation Using Kalman Filtering*. Hoboken, NJ, USA: Wiley, Dec. 2012.
- [23] F. Wirthmüller, M. Klimke, J. Schlechtriemen, J. Hipp, and M. Reichert, "A fleet learning architecture for enhanced behavior predictions during challenging external conditions," in *Proc. SSCI*, vol. 3, Dec. 2020, pp. 2739–2745.
- [24] X. Zhou, X. Zheng, X. Cui, J. Shi, W. Liang, Z. Yan, L. T. Yang, S. Shimizu, and K. I.-K. Wang, "Digital twin enhanced federated reinforcement learning with lightweight knowledge distillation in mobile networks," *IEEE J. Sel. Areas Commun.*, vol. 41, no. 10, pp. 3191–3211, Oct. 2023.
- [25] C. Schwarz and K. Moran, "Digital map enhancements of electronic stability control," *SAE Tech. Paper*, vol. 1, pp. 1–2010, Apr. 2010.
- [26] Z. Hu, S. Lou, Y. Xing, X. Wang, D. Cao, and C. Lv, "Review and perspectives on driver digital twin and its enabling technologies for intelligent vehicles," *IEEE Trans. Intell. Vehicles*, vol. 7, no. 3, pp. 417–440, Sep. 2022.
- [27] L. Yu and R. Wang, "Researches on adaptive cruise control system: A state of the art review," *Proc. Inst. Mech. Eng., D, J. Automobile Eng.*, vol. 236, nos. 2–3, pp. 211–240, Feb. 2022.
- [28] A. Borneo, L. Zerbato, F. Miretti, A. Tota, E. Galvagno, and D. A. Misul, "Platooning cooperative adaptive cruise control for dynamic performance and energy saving: A comparative study of linear quadratic and reinforcement learning-based controllers," *Appl. Sci.*, vol. 13, no. 18, p. 10459, Sep. 2023.
- [29] P. Mandl, F. Jaumann, M. Unterreiner, T. Gräber, F. Klingler, J. Edelmann, and M. Plöchl, "Speed control in the presence of road obstacles: A comparison of model predictive control and reinforcement learning," in *Proc. 16th Int. Symp. Adv. Vehicle Control*, 2024, pp. 91–97.
- [30] Z. Szalay, Z. Hamar, and Á. Nyerges, "Novel design concept for an automotive proving ground supporting multilevel CAV development," *Int. J. Vehicle Design*, vol. 80, no. 1, pp. 1–22, 2019.
- [31] Google. (2024). *GRPC: A High Performance, Open Source Universal RPC Framework*. [Online]. Available: <https://grpc.io/>
- [32] P. Mandl, D. Klein, J. Edelmann, M. Plöchl, and F. Klingler, "Regions of feasible handling in overactuated vehicles considering actuator sets and limits," *Vehicle Syst. Dyn.*, pp. 1–19, Nov. 2025.
- [33] J. Postel, *User Datagram Protocol*, Standard RFC0768, Aug. 1980. [Online]. Available: <https://www.rfc-editor.org/info/rfc0768>
- [34] D. Mills, *Network Time Protocol (Version 3) Specification, Implementation and Analysis*, Standard RFC1305, Mar. 1992. [Online]. Available: <https://www.rfc-editor.org/info/rfc1305>
- [35] J. A. E. Andersson, J. Gillis, G. Horn, J. B. Rawlings, and M. Diehl, "CasADi: A software framework for nonlinear optimization and optimal control," *Math. Program. Comput.*, vol. 11, no. 1, pp. 1–36, Mar. 2019.
- [36] A. Wächter and L. T. Biegler, "On the implementation of an interior-point filter line-search algorithm for large-scale nonlinear programming," *Math. Program.*, vol. 106, no. 1, pp. 25–57, Mar. 2006.
- [37] M. Massaro, S. Lovato, and M. Veneri, "An optimal control approach to the computation of G-G diagrams," *Vehicle Syst. Dyn.*, vol. 62, no. 2, pp. 448–462, Feb. 2024.
- [38] B. Stellato, G. Banjac, P. Goulart, A. Bemporad, and S. Boyd, "OSQP: An operator splitting solver for quadratic programs," *Math. Program. Comput.*, vol. 12, no. 4, pp. 637–672, Dec. 2020.
- [39] L. De Novellis, A. Sorniotti, and P. Gruber, "Wheel torque distribution criteria for electric vehicles with torque-vectoring differentials," *IEEE Trans. Veh. Technol.*, vol. 63, no. 4, pp. 1593–1602, May 2014.
- [40] C. Chatzikomis, A. Sorniotti, P. Gruber, M. Bastin, R. M. Shah, and Y. Orlov, "Torque-vectoring control for an autonomous and driverless electric racing vehicle with multiple motors," *SAE Int. J. Vehicle Dyn., Stability*, vol. 1, no. 2, pp. 338–351, Mar. 2017.



**PHILIPP MANDL** received the M.Sc. degree in mechanical engineering from TU Wien, Vienna, Austria, in 2021, where he is currently pursuing the Ph.D. degree. Since 2022, he has been a Research Assistant with the Institute of Mechanics and Mechatronics within the Research Unit of Technical Dynamics and Vehicle System Dynamics, TU Wien. His research interests include vehicle dynamics, with a particular focus on optimisation-based methods for overactuated vehicles.



**JOHANNES EDELMANN** received the Ph.D. and *venia docendi* degrees in technical dynamics from TU Wien, Austria, in 2008 and 2011, respectively. From 2018 to 2021, he was an Associate Professor with the Institute of Mechanics and Mechatronics, TU Wien. Since 2021, he has been a Professor of technical dynamics with the Institute of Mechanics and Mechatronics. His research interests include applied multibody dynamics, stability of dynamical systems, and vehicle dynamics modeling and control.



**MANFRED PLÖCHL** received the Ph.D. and *venia docendi* degrees in mechanics from TU Wien, Austria, in 1996 and 2001, respectively. Since then, he has been a Professor of mechanics with the Institute of Mechanics and Mechatronics, TU Wien, where he is responsible for a lectures on vehicle dynamics and multibody dynamics. He is an Editor of *Vehicle System Dynamics* and the Secretary General of the International Association for Vehicle System Dynamics (IAVSD).



**FLORIAN KLINGER** received the Ph.D. degree from the Institute of Mechanics and Mechatronics, TU Wien, Austria, in 2018. Since, he has been a Senior Lecturer with the Institute of Mechanics and Mechatronics. His research interests include the modeling of vehicle dynamics, human drivers, and driver assistance systems in the field of micromobility, as well as digital twins in the road domain.

...